Accepted for publication in *Water Resources Research*, Vol. 36, No. 10, pages 2937-2946.

The actual article follows

WATER RESOURCES RESEARCH, VOL. 36, NO. 3, PAGES 725–735, MARCH, 2000

Thermal mediation by littoral wetlands and impact on lake intrusion depth

Hrund Ó. Andradóttir and Heidi M. Nepf

Ralph M. Parsons Laboratory, Department of Civil and Environmental Engineering
Massachusetts Institute of Technology, Cambridge

Abstract. Lake inflow dynamics can be affected by the thermal mediation provided by shallow littoral regions such as wetlands. In this study, wetland thermal mediation is evaluated using a linearized dead-zone model. Its impact on lake inflow dynamics is then assessed by applying the model sequentially to the river reach, wetland, and lake. Our results suggest that littoral wetlands can dramatically alter the inflow dynamics of reservoirs located in small or forested watersheds, for example, by raising the temperature of the inflow during the summer and creating surface intrusions when a plunging inflow would otherwise exist. Consequently, river-borne nutrients, contaminants, and pathogens enter directly into the epilimnion, where they enhance eutrophication and the risk of human exposure. The addition of a littoral wetland has less significant effects in larger watersheds, where the water has already equilibrated with the atmosphere upon reaching the wetland and sun shading is less prominent.

1. Introduction

Littoral wetlands are important transition zones between uplands and deep aquatic systems (Figure 1). Besides having a unique ecosystem, they can improve downstream water quality both through sediment settling and chemical and biological processes [*Johnston et al.*, 1984; *Tchobanoglous*, 1993]. Attempting to harness this filtering capacity, over 300 wetlands have already been constructed in North America to provide cheap, low-maintenance wastewater treatment [*Reed and Brown*, 1992; *Bastian and Hammer*, 1993]. In addition to transforming the chemical and particulate composition of the water, wetlands can also alter the water temperature, such that the temperature of the water leaving the wetland T_W differs from that of the river that feeds it, T_R (see Figure 1). This thermal mediation is especially important in littoral wetlands, where it can alter the intrusion dynamics in a lake and ultimately affect lake water quality.

A recent attempt at eutrophication control for Lake McCarrons in Minnesota provides an instructive example of why one must consider thermal mediation when designing a constructed wetland for water quality improvement. A wetland was constructed to reduce nutrient loads to Lake McCarrons. Although effective in reducing nutrient fluxes, the wetland did not improve the lake water quality, partly because it raised the lake inflow temperature sufficiently during summer months to change its intrusion depth. In particular, after the addition of the wetland, contaminant and nutrient fluxes were carried directly into the lake's epilimnion where they were more damaging (i.e., $T_W \approx T_L$ on Figure 1), instead of plunging into the thermocline as they had before the wetland was built (i.e., $T_W < T_L$ on Figure 1) [*Oberts*, 1998; *Metropolitan Council*, 1997]. Because thermal mediation was not considered in the design, the wetland performance was significantly undermined.

Despite the important implications for lake water quality, wetland thermal mediation remains a relatively unstudied process. To the authors knowledge, fundamental questions such as when and why wetland thermal mediation occurs and how it alters lake intrusion dynamics, have still not been answered. To address these questions, wetland thermal mediation must be considered as a part of an integrated watershed process (Figure 1): First, the degree of thermal mediation provided by a littoral wetland depends on the temperature of the water delivered from the watershed, that is, the river temperature T_R. Second, the impact of wetland thermal mediation on lake water quality depends on the temperature of the wetland outflow T_W, relative to the temperature of the lake epilimnion T_L [*Fisher et al.*, 1979, p. 209]. Therefore, to fully understand this process requires an analysis of both the local thermal processes within the wetland and the global thermal processes across the watershed, that is, determining groundwater temperature T_G, surface runoff temperature T_S, as well as T_R, T_W, and T_L in Figure 1.

By considering the watershed scale, the work presented in this paper goes beyond previous thermal analyses aimed at eutrophication control [e.g., *Harleman*, 1982] and cooling water discharge [e.g., *Jirka et al.*, 1978], both of which focused on small subsections of the watershed. Furthermore, this paper provides a link between thermal mediation in shallow flow-through systems and differential heating and cooling, a process responsible for diurnal exchange flows between the pelagic region of a lake and its shallow stagnant side arms [*Monismith et al.*, 1990; *Farrow and Patterson*, 1993]. The differential heating and cooling pattern is generated because rivers and wetlands are shallower and more enclosed than pelagic regions in lakes. As a result, they distribute heat over shorter depths and experience greater sun shading and wind sheltering, which reduces their exposure to solar, latent, and convective heating [*Sinokrot and Stefan*, 1993].

The goal of this paper is to generate a general analytical framework for evaluating the impact of wetland thermal mediation on lake inflow temperature. Building upon cooling pond analysis [*Jirka et al.*, 1978; *Jirka and Watanabe*, 1980; *Adams*, 1982], a simple conceptual model, called the dead-

Paper number 1999WR900306.
0043-1397/00/1999WR900306$09.00

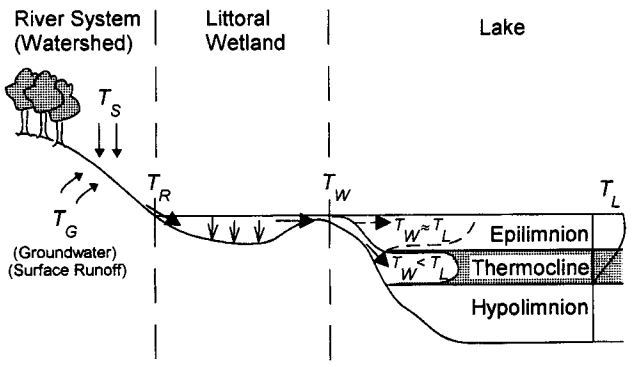

Figure 1. Littoral wetlands are transition zones between uplands and deep aquatic systems. The water temperature evolves from its source (T_G or T_S), down the river reach (T_R), through the wetland (T_W), and into the lake (T_L). If thermal mediation occurs within the wetland, that is, $T_W \neq T_R$, the lake intrusion dynamics may be altered. Specifically, if $T_W \approx T_L$, then surface intrusions occur, whereas if $T_W < T_L$, a plunging inflow occurs.

zone model, is introduced to explore the mechanisms behind wetland thermal mediation and river/wetland-lake interactions. The dead-zone model is presented in section 2. The steady and periodic thermal responses predicted by this model are discussed in section 3. Finally, in section 4 the model is integrated across different watershed subsections, and the results are used to compare the lake intrusion dynamics for systems with and without littoral wetlands. The theoretical results in this paper are verified with field experiments in the work of H. Ó. Andradóttir and H. M. Nepf (Thermal mediation in a natural littoral wetland: Measurements and modeling, manuscript in preparation, 1999) (hereinafter referred to as Andradóttir and Nepf, manuscript in preparation, 1999).

2. Dead-Zone Model

To accurately predict wetland thermal processes, a model must properly reflect the wetland circulation. The water circulation controls the skewness and variance of the residence time distribution (RTD), both of which determine how effectively the water is thermally mediated in the system [*Jirka and Watanabe*, 1980]. Wetland circulation is strongly influenced both by the presence of vegetation and meteorological conditions. In particular, natural wetlands receiving unregulated river inflow are often bimodal, oscillating between two general circulation regimes in response to shifting inflow conditions [*Andradóttir*, 1997; *DePaoli*, 1999]. During low flows, vegetation drag, wind, and buoyancy dominate the water circulation, and the wetland can exhibit a complex three-dimensional flow behavior which varies with the onset and breakdown of stratification and changing wind conditions. However, the integrated effect of these processes over time is that the wetland behaves as a partially well mixed reactor in which the river inflow fills the wetland volume, producing an RTD with a large variance around the nominal residence time $\bar{t}$ (Figure 2a). In contrast, during high flows, river momentum dominates the circulation and short-circuiting occurs; that is, the river trajectory cuts straight across the wetland, with most flow exiting in much less time than the nominal residence time $\bar{t}$, producing a skewed RTD (Figure 2b). Short-circuiting can be enhanced by stationary dead zones created by vegetation and irregular bathymetry [e.g., *Thackston et al.*, 1987].

The dead-zone model is a simple conceptual model, originally developed for river routing and dispersion studies, that accounts for dead-zone trapping by channel irregularities, bed forms, and vegetation [e.g., *Valentine and Wood*, 1977; *Bencala and Walters*, 1983]. In addition, the model can simulate a wide range of circulation regimes, including both the short-circuiting and well-mixed regimes discussed above. For these reasons the dead-zone model is an appropriate choice and adapted here to wetlands. The schematic of the model is presented in Figure 3. The wetland is divided into two zones. The first zone is a flow zone (channel) of mean depth H_c, width W_c, and cross-sectional area, $A_c = W_c H_c$. This zone receives inflow at temperature T_0 and flow rate Q_r that traverses across the wetland at the mean velocity, $u = Q_r/A_c$, and disperses longitudinally with dispersion coefficient D_x. The second zone is a stationary ($u = 0$) dead zone with depth H_d, width W_d, and cross-sectional area, $A_d = W_d H_d$. The two zones communicate with one another through a spatially uniform lateral exchange characterized by the lateral exchange coefficient, $\alpha = \Delta Q/(A_c + A_d)L$, where ΔQ is the total lateral exchange rate between the two zones and L is the length of the wetland. The governing equation for the depth-averaged temperature in the flow zone $T_c(x, t)$ is

$$\frac{\partial T_c}{\partial t} + u\frac{\partial T_c}{\partial x} = D_x\frac{\partial^2 T_c}{\partial x^2} + \frac{\alpha}{q}(T_d - T_c) + \frac{\phi}{\rho C_p H_c} \quad (1)$$

and for the depth-averaged temperature in the dead zone $T_d(x, t)$ is

$$\frac{\partial T_d}{\partial t} = -\frac{\alpha}{1-q}(T_d - T_c) + \frac{\phi}{\rho C_p H_d}, \quad (2)$$

where $q = A_c/(A_c + A_d)$ is the jet areal ratio, $\phi(t)$ is the net surface heat flux per surface area, ρ is the density, and C_p is the

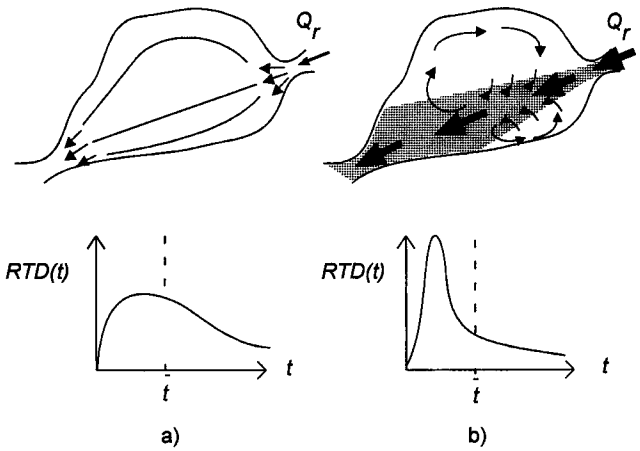

Figure 2. Schematic of circulation regimes and residence time distributions (RTD) in free water surface wetlands. (a) Water circulation dominated by vegetation drag, wind, and buoyancy. The wetland behaves as a partially well-mixed reactor, corresponding to an RTD with a large variance around the mean nominal residence time $\bar{t}$. (b) River-dominated circulation with a distinct flow region (dark shaded area). Short circuiting occurs, producing a skewed RTD with much of the flow exiting the wetland in less time than $\bar{t}$.

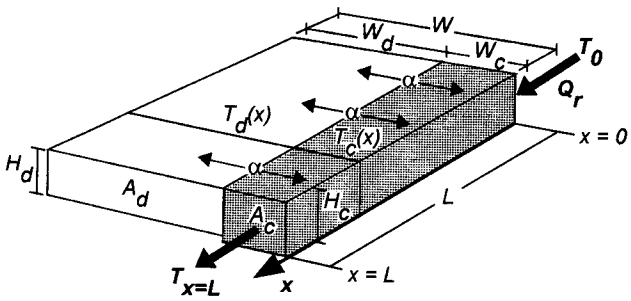

Figure 3. Schematic of the dead-zone model. The wetland is divided into a channel or flow zone (shaded area) and stationary dead zone. These two zones communicate with one another through spatially uniform lateral water exchange α (s^{-1}). Thermal mediation within the wetland is reflected in $T_{x=L} \neq T_0$.

specific heat of water. To ensure heat conservation, the boundary conditions are

$$uT_c(0, t) - D_x \left.\frac{\partial T_c}{\partial x}\right|_{x=0} = uT_0(t)$$
$$\left.\frac{\partial T_c}{\partial x}\right|_{x=L} = 0. \tag{3}$$

The net surface heating is the sum of five heat fluxes:

$$\phi = (1 - R)S + \phi_1 + \phi_2 + \phi_S + \phi_L, \tag{4}$$

where S is the incoming solar (short wave) radiation, R the reflection coefficient, ϕ_1 is the incoming long wave radiation, ϕ_2 is the back radiation, ϕ_S is the sensible (conductive) heat flux, and ϕ_L is the latent (evaporative) heat flux. Many empirical expressions exist for each one of these terms, and the resulting equation is a nonlinear function of both water temperature and atmospheric conditions such as air temperature, wind speed, relative humidity, and cloud cover [e.g., *Fisher et al.*, 1979, p. 163]. These heat flux estimates may need to be modified to account for sun shading and wind sheltering, which can occur in rivers as well as wetlands because of emergent vegetation, borderline trees, and nearby hills.

In order to derive analytical solutions, ϕ can be linearized using the concept of an equilibrium temperature T_E, defined as the temperature for which the water is at equilibrium with atmospheric conditions such that the net surface heat flux equals zero [*Edinger and Geyer*, 1965], that is,

$$\frac{\phi}{\rho C_p H} = \frac{K}{H}(T_E - T). \tag{5}$$

The surface heat transfer coefficient K represents the rate of surface heating and cooling and varies temporally with meteorological conditions (in particular wind speed) and surface water temperature [e.g., *Ryan et al.*, 1974]. This coefficient generally lies between 0.4 and 1.0 m/d for low winds (<2 m/s), increasing to 0.8–2.0 m/d for high winds (8 m/s) [*Ryan et al.*, 1974]. The ratio $t_{\text{heat}} = H/K$ is the timescale of vertical heat transfer and represents the thermal inertia of the water column, which is a measure of how rapidly the system responds to changes in atmospheric forcing and how much heat it stores. Shallow systems with low thermal inertia can more readily track changing atmospheric conditions but store less heat than deep systems; that is, as $H \to 0$, then $t_{\text{heat}} \to 0$ and $T \to T_E$.

Finally, (5) is an exact representation of the surface heat flux if the heat transfer coefficient K is allowed to vary in time. For mathematical simplicity, however, K will be taken as constant following *Jirka and Watanabe* [1980] and *Adams* [1982]. This is a reasonable approximation except when the water temperature deviates substantially from the equilibrium temperature [*Yotsukura et al.*, 1973], as occurs when the timescale of variation for T_E is short compared to t_{heat}, for example, over synoptic and diurnal timescales.

3. Exploration of General Results

Temperature variations in shallow water are driven by meteorological changes that occur predominantly on three timescales, that is, diurnal (P = 1 day), synoptic (P = 1–2 weeks), and seasonal (P = 1 year) [*Adams*, 1982]. To explore these multiple timescales of variations, the meteorological forcing, T_E, and temperature of the wetland inflow (at $x = 0$) T_0 are assumed to be sinusoidal with period P, that is,

$$T_E = \bar{T}_E + \Delta T_E e^{i2\pi t/P}, \tag{6}$$

$$T_0 = \bar{T}_0 + \Delta T_0 e^{i2\pi t/P}. \tag{7}$$

With this input the linearized dead-zone model (equations (1)–(5)) is solved for the water temperature in the wetland channel (c) and dead zone (d) in the form

$$T_{c,d} = \bar{T}_{c,d} + \Delta T_{c,d} e^{i2\pi t/P}. \tag{8}$$

Here $\bar{T}_i$ represents the steady and ΔT_i represents the periodic component of these sinusoidal temperature cycles. The periodic component $\Delta T_i = |\Delta T|_i e^{-i2\pi\theta_i/P}$ incorporates both the amplitude $|\Delta T|_i$ and time lag θ_i between the water and equilibrium temperatures (i.e., $\theta_E = 0$). To get familiar with this notation, consider Figure 4, which displays typical thermal cycles at the inlet (T_0) and outlet ($T_{x=L}$) of a wetland responding to seasonal and diurnal meteorological forcing (T_E). On seasonal timescales (Figure 4a) the wetland thermally mediates the water temperature, such that $T_{x=L} \neq T_0$. Specifically, the time lag is reduced (i.e., $\theta_{x=L} < \theta_0$), and the amplitude of thermal oscillation is increased (i.e., $|\Delta T|_{x=L} > |\Delta T|_0$). On a day-to-day basis (Figure 4b) this seasonal thermal mediation appears as a difference in the mean temperature between the inlet (15°C) and the outlet (21°C) water of the wetland. Notice that although the wetland also mediates the diurnal thermal response, that is, $|\Delta T|_{x=L} > |\Delta T|_0$ and $\theta_{x=L} < \theta_0$ on Figure 4b, this diurnal thermal mediation does not significantly add to the seasonal thermal mediation, which dominates during large portions of the year (e.g., J.D. 50–250 and 300–365 on Figure 4a). Finally, Figure 4b illustrates that the wetland water is unable to track the diurnal meteorological changes (i.e., $\Delta T_E \gg |\Delta T|_{x=L}$ and $\theta_{x=L} \approx 6$ hours $= P/4$), which leads to differential heating and cooling as will be discussed in more detail in section 3.2. To summarize, Figure 4 demonstrates that to fully understand the impact of wetlands, both diurnal and seasonal responses must be considered.

3.1. Steady Response

The steady state response of the wetland is found by solving the governing equations (1) and (2) with $\partial T_{c,d}/\partial t = 0$. Assuming u, D_x, K, and α are constant in space and time, the solution for the flow zone temperature can be written as

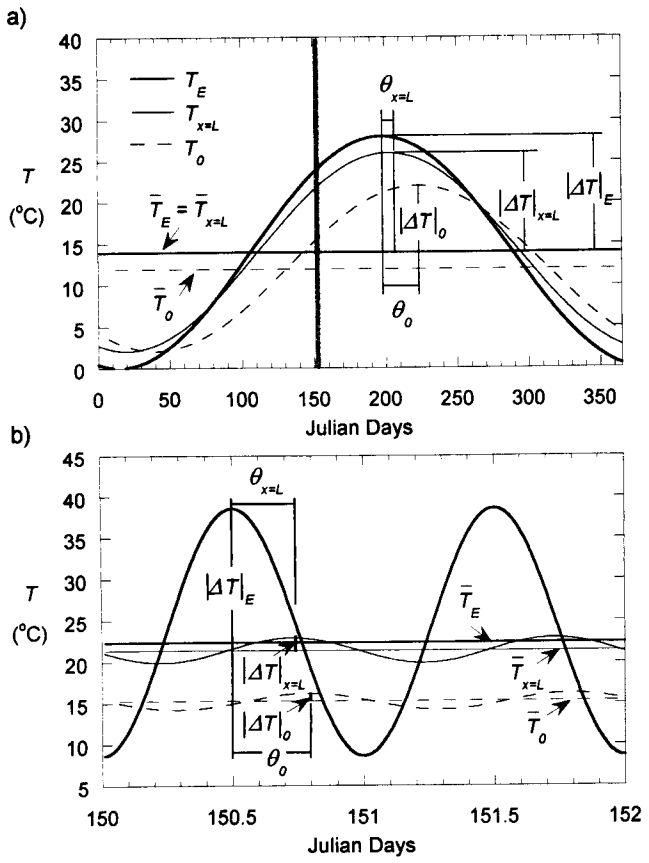

Figure 4. Thermal cycles at the inlet T_0 and outlet $T_{x=L}$ of a wetland, forced by changes in the equilibrium temperature T_E. (a) Seasonal cycle (P = 1 year) and (b) diurnal cycle (P = 1 day) during early June (Julian day = 150–152) in North America, when the inflow is, on average, colder than the outflow. Thermal mediation occurs both on seasonal and diurnal timescales.

$$\frac{\bar{T}_c - \bar{T}_0}{\bar{T}_E - \bar{T}_0} = 1 - 2\frac{(1-a)\exp\left[\frac{1}{2E^*}(1+a)\frac{x}{L}\right] - (1+a)\exp\left[\frac{a}{E^*} + \frac{1}{2E^*}(1-a)\frac{x}{L}\right]}{(1-a)^2 - (1+a)^2\exp\left(\frac{a}{E^*}\right)}, \tag{9}$$

where $a = \sqrt{1 + 4E^* b_S}$ and

$$b_S = r\left[\frac{\alpha^*(1-w)}{\alpha^* + (1-w)r} + w\right]. \tag{10}$$

Here b_S represents the effective thermal capacity of the wetland, the details of which are discussed later in this section. The solution for the dead-zone temperature is

$$\frac{\bar{T}_d}{\bar{T}_E} = \frac{\alpha^* \frac{\bar{T}_c}{\bar{T}_E} + (1-w)r}{\alpha^* + (1-w)r}. \tag{11}$$

The steady response of the wetland is thus governed by four nondimensional parameters:

r nominal thermal capacity, equal to $\bar{t}/\bar{t}_{\text{heat}} = KWL/Q_r$;
E^* dispersion number (or inverse Peclet number), equal to D_x/uL;
α^* nondimensional lateral exchange coefficient, equal to $\alpha\bar{t} = \Delta Q/Q_r$;
w width ratio, equal to W_c/W.

The thermal capacity r reflects the heating/cooling potential of the system. It is defined as the ratio between the nominal residence time, $\bar{t} = (A_c + A_d)L/Q_r$, and nominal thermal inertia, $\bar{t}_{\text{heat}} = K/H$, where H is the average wetland depth. Notice that although both $\bar{t}$ and $\bar{t}_{\text{heat}}$ are functions of depth, the thermal capacity, $r = \bar{t}/\bar{t}_{\text{heat}}$, is not. The three remaining parameters, E^*, α^*, and w, define the hydraulic or circulation regime within the wetland and control the shape of the residence time distribution RTD (see Figure 2). The dispersion number E^* describes the relative importance of longitudinal dispersion and advection. The lateral exchange coefficient α^* represents the fractional water exchange between the flow and dead zone (i.e., $\Delta Q/Q_r$) and describes the relative importance of lateral exchange and advection. The width ratio w describes the size of the flow zone relative to the total wetland and is related to the jet areal ratio, that is, $w = q/(H_c/H)$. If the wetland has uniform water depth, that is, $H = H_c = H_d$, then $w = q$.

The dependence of the steady solution (9) with respect to E^* is the same as the one-dimensional, longitudinal dispersion model. In general, increasing the longitudinal dispersion E^* reduces the degree of thermal mediation within the system. A more detailed description of this dependence is given by, for example, *Jirka and Watanabe* [1980] and will not be repeated here. Instead, for simplicity, we assume $E^* = 0$ and use this subcase to explore the remaining governing parameters and their effect on wetland thermal mediation. This simplification does not strictly limit the model, as short-circuiting, shear flow dispersion, and plug flow can all be represented with $E^* = 0$ (see the Appendix), and the general trends described here apply for $E^* \neq 0$ as well.

The dependence of the steady solution (9) on the parameters, r, α^*, and, w is illustrated in Figure 5 for $E^* = 0$. The degree of thermal mediation is given by the ratio $(\bar{T}_{x=L} - \bar{T}_0)/(\bar{T}_E - \bar{T}_0)$, which represents the actual change in temperature between the inlet and outlet of the wetland, $\bar{T}_{x=L} - \bar{T}_0$, relative to the maximum potential change, $\bar{T}_E - \bar{T}_0$, which would occur if thermal equilibrium with the atmosphere were reached. As shown on Figure 5, the thermal capacity r controls the degree of thermal mediation provided by a wetland. For $r \ll 1$, the residence time limits the heat capture, and no thermal mediation occurs, that is, $\bar{T}_{x=L} = \bar{T}_0$. For $r \gg 1$, however, the residence time is not limiting, and the outflow temperature reaches equilibrium with atmospheric conditions, that is, $(\bar{T}_{x=L} - \bar{T}_0)/(\bar{T}_E - \bar{T}_0) = 1$. The rate with respect to r at which the thermal mediation curves approach equilibrium is described as the thermal efficiency and depends on the hydraulic parameters α^* and w. The most efficient flow regime is plug flow (dotted-dashed curve on Figure 5), which is equivalent to $\alpha^* \to \infty$ given $E^* = 0$ and for which $b_S = r$. For other flow regimes the effective thermal capacity of the wetland b_S is smaller than the nominal thermal capacity r. In particular, (10) shows that

$$\underset{\alpha^*=0}{wr} \leq b_S \leq \underset{\alpha^*\to\infty}{r},$$

which indicates that a large dead zone (small w) and a small exchange flow (small α^*) both reduce the effective thermal capacity of the wetland such that $b_S \ll r$. Such systems have low thermal efficiency, that is, produce less thermal mediation at any value of r (Figures 5a and 5b), because only a fraction of the nominal thermal capacity r is utilized to mediate the water temperatures. As either α^* or w increase, $b_S \rightarrow r$ because the dead zone contributes more actively to the thermal mediation. Such systems are more laterally homogeneous, $\bar{T}_c \rightarrow \bar{T}_d$, and have higher thermal efficiency, that is, produce more thermal mediation at any value of r (Figures 5a and 5b). As a result of this dependence on α^* and w, both short-circuiting flow ($\alpha^* w \lesssim H/H_c$) and stirred reactor-type flow (dashed curve on Figure 5) are less efficient than shear flow with dispersion ($\alpha^* w \gtrsim H/H_c$). This is in agreement with previous analysis of steady cooling pond performance [*Jirka and Watanabe*, 1980].

Finally, the impact of short-circuiting based on a dead-zone model with a uniformly distributed lateral exchange, as presented here, differs from previous recirculation models of short-circuiting [*Jirka and Watanabe*, 1980], which assume that the exchange flow ΔQ enters the channel at a discrete location near the entrance of the wetland and recirculates back to the dead zone near the outlet (see Figure 6a). The steady state solutions from both models are compared on Figure 6b. For a given exchange flow ratio $\Delta Q/Q_r$ and jet areal ratio w (or q),

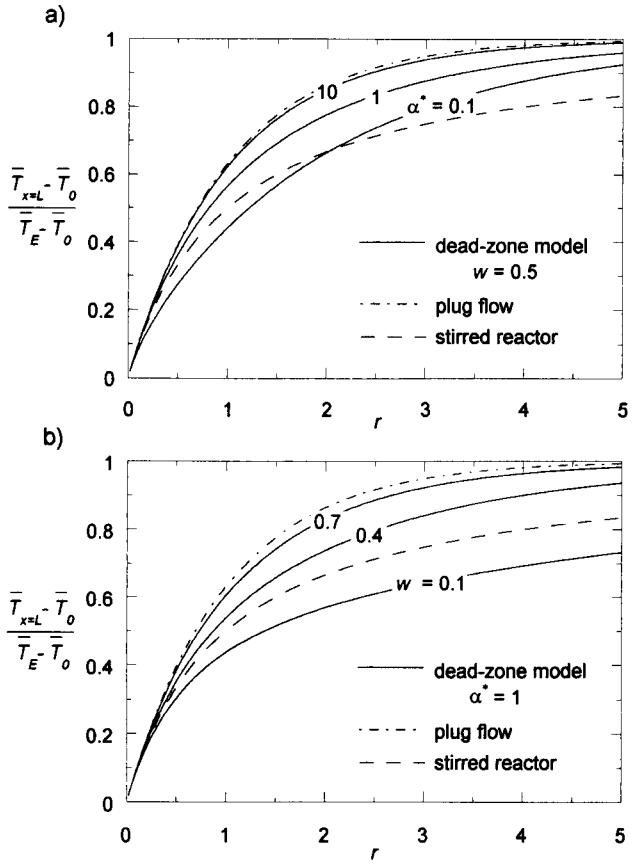

Figure 5. Steady dead-zone model results as a function of thermal capacity r for $E^* = 0$. (a) Variable α^* with $w = 0.5$ and (b) variable w with $\alpha^* = 1$. Increasing α^* and/or w improves the thermal efficiency; that is, more thermal mediation $(\bar{T}_{x=L} - \bar{T}_0)/(\bar{T}_E - \bar{T}_0)$ is achieved at any given r.

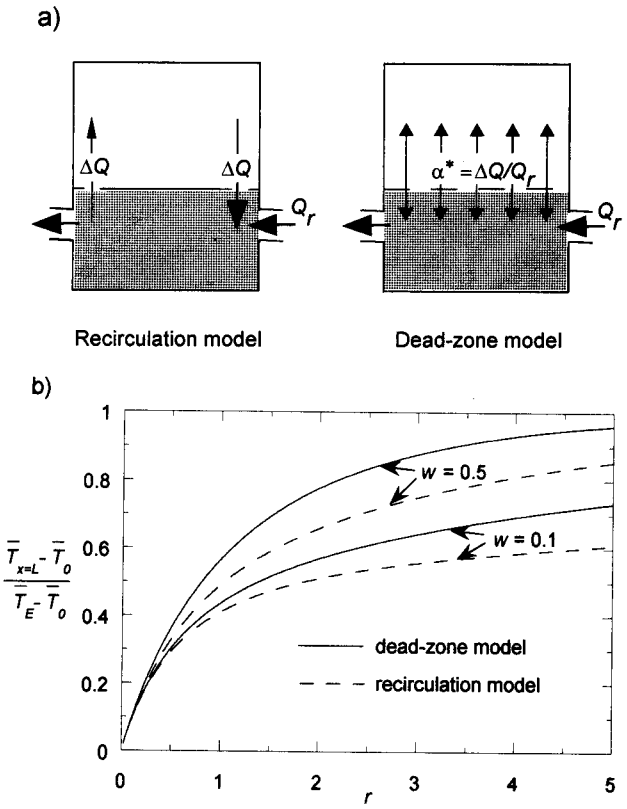

Figure 6. Comparison between short-circuiting predicted by the dead-zone model and the recirculation model [*Jirka and Watanabe*, 1980]. (a) Schematic of both models. (b) Steady thermal mediation with respect to w and r ($\Delta Q/Q_r = 1$ and $E^* = 0$). The recirculation model predicts consistently less thermal mediation than the dead-zone model.

the recirculation model consistently predicts less thermal mediation than the dead-zone model. Actual wetlands will tend to fall between these two models, displaying a combination of lateral exchange and basin-scale recirculation. In particular, sparsely vegetated wetlands with a large length-to-width ratio (Figure 2b) are likely to contain some degree of recirculation [*Jirka et al.*, 1978; *Thackston et al.*, 1987]. This tendency to recirculate is reduced by uniform vegetation drag [*Wu and Tsanis*, 1994], which exerts a stabilizing effect on large-scale eddies [*Babarutsi et al.*, 1989], and uneven vegetation which generates preferential flow paths. Consequently, the dead-zone model is expected to realistically capture short-circuiting in densely/unevenly vegetated wetlands but may slightly overpredict thermal mediation in sparsely vegetated wetlands.

3.2. Periodic Response

The periodic response is considered relative to the equilibrium temperature, that is,

$$\Gamma_j = \Delta T_j/\Delta T_E = |\Gamma|_j\, e^{-i2\pi\theta_j/P} \qquad j = c,\ d,\ 0,$$

where Γ_j incorporates the relative amplitude $|\Gamma|_j$ and time lag θ_j between the water and equilibrium temperature. Both $|\Gamma|_j$ and θ_j reflect the degree to which equilibrium with the atmosphere is reached (see Figure 4). The analytical solution of (1)–(5) for the wetland flow zone is

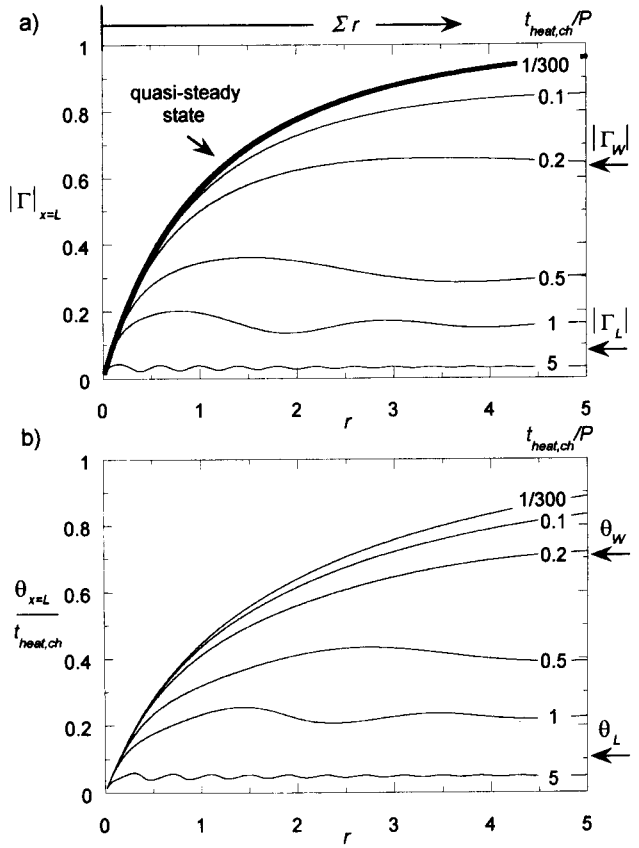

Figure 7. Periodic dead-zone model results as a function of r and $t_{\text{heat,ch}}/P$ with $E^* = 0$, $\alpha^* = 1$, $w = 0.5$, $H_c/H = 1$, and $\Gamma_0 = 0$. (a) Nondimensionalized amplitude $|\Gamma|_{x=L}$. (b) Time-lag $\theta_{x=L}/t_{\text{heat,ch}}$ between the outlet and equilibrium temperature. The periodic thermal response becomes more damped as $t_{\text{heat,ch}}/P$ increases.

$$\frac{\Gamma_c - \Gamma_0}{\Gamma^* - \Gamma_0} = 1 - 2\frac{(1-a)\exp\left[\frac{1}{2E^*}(1+a)\frac{x}{L}\right] - (1+a)\exp\left[\frac{a}{E^*} + \frac{1}{2E^*}(1-a)\frac{x}{L}\right]}{(1-a)^2 - (1+a)^2\exp\left(\frac{a}{E^*}\right)}, \tag{12}$$

where $a = \sqrt{1 + 4E^* b_P}$,

$$b_P = \frac{\alpha^* r\left[(1-w) + i2\pi\left(1 - w\frac{H_c}{H}\right)\frac{\bar{t}_{\text{heat}}}{P}\right]}{\alpha^* + r\left[(1-w) + i2\pi\left(1 - w\frac{H_c}{H}\right)\frac{\bar{t}_{\text{heat}}}{P}\right]} + wr\left(1 + i2\pi\frac{H_c}{H}\frac{\bar{t}_{\text{heat}}}{P}\right) \tag{13}$$

$$b_P = r\left(1 + i2\pi\frac{\bar{t}_{\text{heat}}}{P}\right)\cdot\left[w + \frac{\alpha^*(1-w)}{\alpha^* + r(1-w)\left(1 + i2\pi\frac{\bar{t}_{\text{heat}}}{P}\right)}\right] \qquad \frac{H_c}{H} = 1, \tag{14}$$

$$\Gamma^* = \left\{\alpha^* + wr\left[(1-w) + i2\pi\left(1 - w\frac{H_c}{H}\right)\frac{\bar{t}_{\text{heat}}}{P}\right]\right\}\cdot\left\{wr\left(1 + i2\pi\frac{H_c}{H}\frac{\bar{t}_{\text{heat}}}{P}\right)\left[(1-w) + i2\pi\cdot\left(1 - w\frac{H_c}{H}\right)\frac{\bar{t}_{\text{heat}}}{P}\right] + \alpha^*\left(1 + i2\pi\frac{\bar{t}_{\text{heat}}}{P}\right)\right\}^{-1} \tag{15}$$

$$\Gamma^* = \frac{1}{1 + i2\pi\dfrac{\bar{t}_{\text{heat}}}{P}} \qquad \frac{H_c}{H} = 1. \tag{16}$$

Here Γ^* represents the asymptotic state under periodic forcing, that is, $\Gamma^c \to \Gamma^*$ as $r \gg 1$. The periodic solution for the dead zone is

$$\Gamma_d = \frac{\alpha^*\Gamma_c + (1-w)r}{\alpha^* + r\left[(1-w) + i2\pi\left(1 - w\frac{H_c}{H}\right)\frac{\bar{t}_{\text{heat}}}{P}\right]}. \tag{17}$$

The periodic solution has the same form as the steady solution, as seen by comparing (12) to (9). As with the steady response, thermal mediation generally increases as r, α^*, and w increase. The important difference between the periodic and steady solutions arises from the additional dependence on the timescale ratio $[(H_c/H)\bar{t}_{\text{heat}}]/P$ appearing in (13), (15), and (17), which compares the thermal inertia of the channel,

$$t_{\text{heat,ch}} = \frac{H_c}{H}\bar{t}_{\text{heat}} = \frac{H_c}{K},$$

to the period of the forcing P. This timescale ratio controls the degree to which the periodic heat capture of a wetland is limited by the thermal inertia of the flow zone $t_{\text{heat,ch}}$. This dependence is illustrated in Figure 7, which displays the periodic thermal mediation with respect to r for different values of $t_{\text{heat,ch}}/P$. For simplicity, the solution assumes a constant inflow temperature, $\Gamma_0 = 0$, and $E^* = 0$. Figure 7 shows that as r increases, the wetland response loses its dependency on r and approaches the state of a stationary water body [*Adams*, 1982], that is,

$$|\Gamma|_{x=L} \xrightarrow{r \gg 1} \frac{1}{\sqrt{(2\pi t_{\text{heat,ch}}/P)^2 + 1}} \tag{18}$$

$$\theta_{x=L} \xrightarrow{r \gg 1} \frac{\tan^{-1}(2\pi t_{\text{heat,ch}}/P)}{2\pi/P}. \tag{19}$$

Consequently, the periodic thermal mediation for $r \gg 1$ is solely determined by $t_{\text{heat,ch}}/P$. When $t_{\text{heat,ch}}/P$ is large, the wetland is unable to track the atmospheric forcing, because the forcing varies more rapidly than the wetland can respond. This results in decreasing values of $|\Gamma|_{x=L}$ and $\theta_{x=L}/t_{\text{heat,ch}}$ as seen in Figure 7. Furthermore, for large $t_{\text{heat,ch}}/P$ the timescale ratio $wr(H_c/H)\bar{t}_{\text{heat}}/P = [wrt_{\text{heat,ch}}]/P$ that appears in (13) also becomes large. As a result, the residence time in the channel $wrt_{\text{heat,ch}}$ limits the fraction of the heating cycle the wetland captures, producing oscillations in $|\Gamma|_{x=L}$ and $\theta_{x=L}$ relative to r (see Figure 7, $t_{\text{heat,ch}}/P = 1, 5$). Finally, for small $t_{\text{heat,ch}}/P$ the thermal inertia is not limiting, and the wetland is at quasi steady state with the forcing. Consequently, if r is large enough,

Table 1. Typical Ranges of Dead-Zone Model Parameters for Rivers, Wetlands, and Surface Layers of Lakes under Nonstorm Conditions

	$\bar{t}$	H, m	E^*	α^*	q	t_{heat}, days	r
Rivers	hours to month (1)	0.1–10 (1)	0.005–0.08 (2,3)	0.1–0.8 (2)	0.25–0.95 (2,4)	0.1–20	1–5
Wetlands	days to month (5,6)	0.1–2 (6,7)	...	0–4 (5)	0.5–0.7 (5)	0.1–2	2–20
Lakes	week to years (8)	2–100 (9)	...	...	...	2–100	2–20

Sources are as follows: (1) *Leopold et al.* [1992, p. 142, 240–242], (2) *Bencala and Walters* [1983], (3) *Day* [1975], (4) *Yu and Wenzhi* [1989], (5) *Kadlec* [1994], (6) *Wood* [1995], (7) *Mitsch and Gosselink* [1993, p. 620], (8) *Fisher et al.* [1979, p. 148], and (9) *Hutchinson* [1957, p. 460]. Ellipsis indicates data are not available.

the wetland tracks the atmospheric fluctuations, that is, $|\Gamma|_{x=L} \rightarrow 1$ but with a lag, $\theta_{x=L} \rightarrow t_{heat,ch}$.

The dependence of the periodic thermal response on $t_{heat,ch}/P$ has two important implications. First, in a given water system the seasonal response (P = 365 days) will significantly differ from both the synoptic (P = 7–14 days) and diurnal (P = 1 day) responses. For example, the seasonal response can be at equilibrium with atmospheric conditions (e.g., $|\Gamma|_{x=L} \approx 1$ for $r \gg 1$), while the synoptic response is partially dampened (e.g., $0.25 < |\Gamma|_{x=L} < 0.85$ for $r > 1$) and the diurnal response is severely dampened (e.g., $|\Gamma|_{x=L} < 0.25$). The system portrayed in Figure 4 demonstrates this difference in seasonal and diurnal response. The second implication is that for a given P, the thermal response of shallow (small $t_{heat,ch}$) and deep (large $t_{heat,ch}$) systems can vary significantly, potentially producing intrusion depth variability and exchange flows. This process is generally referred to as differential heating and cooling (see section 1). For example, consider a 1 m deep wetland ($t_{heat,ch}$ = 2 days) and a 10 m deep lake ($t_{heat,ch}$ = 20 days) with negligible inflow (i.e., $r \gg 1$). On synoptic timescales (P = 10 days) the amplitude response of the wetland, $|\Gamma_W| \approx 0.6$, is much larger than that of the lake, $|\Gamma_L| \approx 0.1$ (see Figure 7a). However, the time lag between the water and equilibrium temperatures is of the same order of magnitude in both systems, that is, $\theta_W = 0.7t_{heat,ch} =$ 1.4 day and $\theta_L = 0.1t_{heat,ch} = 2$ days (see Figure 7b). Similar trends occur on diurnal timescales (P = 1 day), that is, $|\Gamma_W| \approx 0.1$ and $|\Gamma_L| \approx 0.01$, and a time lag of 6 hours. Consequently, the water in the wetland warms more over the day and synoptic heating periods and cools more at night and during synoptic cooling. This differential heating/cooling will affect the intrusion depth variability, as discussed in section 4.2, and may also produce exchange flows, as described by *Monismith et al.* [1990] and *Farrow and Patterson* [1993]. While the dead-zone model can predict when these exchange flows occur, it does not account for their effect on wetland thermal mediation. Finally, on seasonal timescales (P = 365 days) both the wetland and lake are at quasi steady state with the forcing, that is, $|\Gamma_W| \approx |\Gamma_L| \approx 1$. However, the lake lags the wetland because of its larger thermal inertia, producing another form of differential heating/cooling.

4. Wetland Impact on Lake Inflow

To understand the impact of littoral wetlands on lake water quality, the wetland response must be considered in the context of the thermal processes in the watershed. This watershed-scale analysis involves tracing the thermal evolution of the water starting at its source, along the river reach, through the wetland and into the lake (see Figure 1). In section 4.2 this analysis is used to determine when a wetland can significantly impact lake intrusion dynamics.

4.1. Watershed-Scale Analysis

The watershed-scale analysis consists of four steps. First, the thermal properties of the water source must be defined. During nonstorm conditions the water in the river usually originates from groundwater recharge. Because of the thermal inertia of the ground, the seasonal temperature variations of groundwater are severely damped, $|\Gamma_G| \approx 0.2$–0.4, and can lag the equilibrium temperature by 2–4 months (e.g., based upon *Gu et al.* [1996]). Shorter timescale variations (e.g., diurnal and synoptic) are even more dampened such that $|\Gamma_G| \approx 0$. During storms, however, river water originates predominantly from surface runoff, which typically is close to equilibrium with both seasonal and synoptic atmospheric cycles.

Second, the equilibrium temperature T_E must be defined. The equilibrium temperature is a function of both incoming solar radiation and wind. During the summer when leaf cover is peaking, narrow rivers and wetlands experience sun shading and wind sheltering that can give them a different equilibrium temperature than open water (e.g., lakes). While the two processes have a counteracting effect, that is, sun shading reducing T_E but wind sheltering increasing T_E, the sun shading effect is generally more pronounced [*Sinokrot and Stefan*, 1993], yielding a lower equilibrium temperature for narrow systems than for open water.

Third, the model parameters, $\bar{t}$, $\bar{t}_{heat}$, E^*, α^*, and q must be determined for each subsection of the watershed. These parameters are site-specific and depend upon the system's size and shape, the amount and type of vegetation, and the meteorological conditions. The hydraulic parameters E^*, α^*, and q are generally evaluated by conducting dye experiments [*Kadlec*, 1994; *Bencala and Walters*, 1983], whereas the nominal parameters $\bar{t} = WHL/Q_r$ and $\bar{t}_{heat} = H/K$ can be estimated from maps and flow measurements. For a river system which is fed by groundwater/surface runoff throughout its entire reach, the river network residence time can be estimated from the river catchment area A_W and the river discharge at the wetland/lake Q_r. Assuming that the average travel length in the river scales on $\sqrt{A_W}$ and the spatially averaged flow along the reach is $Q_r/2$, then $\bar{t} \approx 2WK\sqrt{A_W}/Q_r$. A representative range for these input parameters under nonstorm conditions is given in Table 1 for each watershed subsection. The parameter values indicate that wetlands are transition zones between the upland and deep aquatic systems, with a small thermal inertia, $t_{heat,ch}$, like rivers but a large thermal capacity r like lakes.

Finally, with the appropriate choice of input parameters the dead-zone model solutions (12)–(16) can be applied sequentially to each watershed subsection. As shown in Figure 8, the

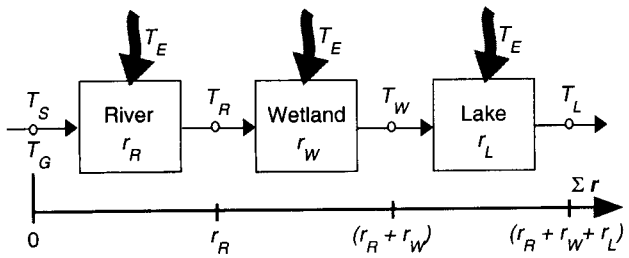

Figure 8. Schematic of the watershed-scale analysis. The dead-zone model is applied to each subsection of a watershed, using the outflow temperature of the previous subsection as the inflow temperature for the next subsection.

outflow temperature from the previous subsection becomes the inflow temperature for the next subsection, that allows tracing the thermal evolution of the surface water from its source, T_G or T_S, to the end of the river reach T_R, to the wetland outflow T_W, and into the lake epilimnion T_L. For simplicity, the vertical heat transfer between the epilimnion and hypolimnion of a lake is neglected. Since this heat transfer is a slow process occurring over months, this assumption introduces errors only at the seasonal timescale but not on the shorter timescales.

4.2. Wetland Impact Scenarios

The thermal evolution presented in Figure 8 depends upon three factors: The first is the equilibrium temperature T_E, and the second is the thermal inertia of the water $t_{\text{heat,ch}}$; together they determine the asymptotic thermal state of surface water. This state may differ across the watershed because of sun shading and wind sheltering and variable water depth. The third factor is the cumulative thermal capacity Σr, which represents the total time that the surface water has been exposed to atmospheric heating relative to the thermal inertia. As Σr increases, the surface water approaches its asymptotic state. In the following we consider the impact of a wetland on lake intrusion dynamics first during low-flow conditions, when the river is predominantly groundwater fed. Then we consider a storm scenario, when the river is predominantly fed by surface runoff. For simplicity, the effects of suspended sediments and salinity on lake intrusion dynamics are neglected.

4.2.1. Nonstorm scenario 1. First, consider a system where the thermal capacity of the river alone is not large enough for it to reach its asymptotic state, that is, $r_R \approx 2WK\sqrt{A_W}/Q_r < 3$ (Figure 7) or where sun shading and wind sheltering are prominent. This generally applies to small watersheds (small A_W) with a high annual discharge (large Q_r) or narrow rivers obstructed by trees or hills. In both cases the water temperature at the end of the river reach T_R will differ from that in the wetland, T_W, and lake, T_L. Figure 9 illustrates simulated thermal cycles in one such system with $r_R = 1$ and $r_W = r_L = 2$. For simplicity, the equilibrium temperature of the river, wetland, and lake is assumed to be the same. First, consider the system without a littoral wetland. On seasonal timescales (P = 365 days), Figure 9a shows that the river water retains the attenuated amplitude and lag ($|\Delta T_R| \approx 9.5$°C and θ_R = 11 days) originating from the damped groundwater source (see section 4.1). In contrast, the lake epilimnion with its long cumulative thermal capacity $\Sigma r > 3$ is almost at equilibrium with the seasonal cycle ($|\Delta T_L| \approx |\Delta T_E| = 15$°C and θ_L = 9 days). Consequently, the river water is colder than the surface waters of the lake during the summer ($T_R < T_L$ for J.D. = 100–280) and is warmer in winter ($T_R > T_L$ for J.D. = 0–100 and 280–365). On diurnal and synoptic timescales (P = 1, 10 days), Figure 9b shows that the thermal response of the shallower river ($t_{\text{heat,ch}}$ = 1 day) is more pronounced than that of the lake ($t_{\text{heat,ch}}$ = 10 days). However, this differential heating and cooling does not produce variability in intrusion depth during the summer period shown because of the large seasonal difference between the river and lake; that is, $T_R < T_L$ in spite of the diurnal and synoptic river temperature fluctuations. Thus in the absence of a littoral wetland the lake intrusion depth varies predominantly on seasonal timescales, the inflow plunging into the hypolimnion during summer and inserting at the surface during winter.

Next consider the impact of adding a littoral wetland to this system. The wetland provides extra thermal capacity allowing the water to reach its asymptotic state. The amplitude of the seasonal temperature cycle of the lake inflow increases from $|\Delta T_R| \approx 9.5$°C to $|\Delta T_W| \approx 15$°C, as the cumulative thermal capacity increases from $\Sigma r = r_R = 1$ to $\Sigma r = (r_R + r_W) = 3$. Consequently, the temperature of the wetland outflow T_W tracks the seasonal temperature cycle in the lake T_L more closely than the river does, reducing the seasonal variability in

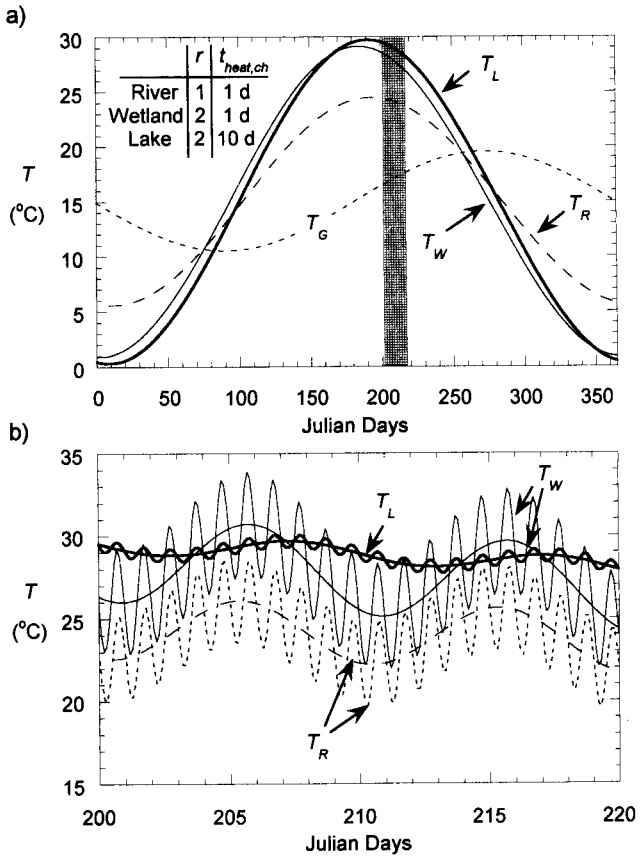

Figure 9. Nonstorm wetland impact scenario 1: r_R = 1. Dead-zone model solutions for a river, T_R, wetland, T_W, and lake epilimnion, T_L, originating from groundwater with the seasonal cycle $\bar{T}_G$ = 15°C, $|T_G|$ = 5°C, and θ_G = 3 months [*Gu et al.*, 1996]. (a) Seasonal (P = 365 days) and (b) synoptic (P = 10 days) and diurnal (P = 1 day) responses. The addition of a littoral wetland can drastically change the lake intrusion dynamics, shifting the variation from predominantly seasonal to predominantly diurnal/synoptic.

intrusion depth (Figure 9a). On diurnal and synoptic timescales (Figure 9b) the wetland heats and cools more rapidly and thus has larger temperature oscillations than the lake, that is, $|\Delta T_W| \gg |\Delta T_L|$. With the seasonal temperature difference reduced, this process now produces diurnal and synoptic variability in the lake intrusion depth, where $T_W > T_L$ over the day and $T_W < T_L$ at night during periods of synoptic heating (J.D. = 202–207 and 212–217).

To summarize, the introduction of a littoral wetland to a watershed where the thermal capacity of the river is small or sun shading/wind sheltering are prominent can drastically change the lake inflow dynamics. Specifically, the variability in intrusion depth is shifted from being predominantly seasonal (no wetland) to occurring predominantly on diurnal and synoptic timescales. Consequently, during the summer, more inflow will be directed toward the lake surface, potentially degrading the lake water quality. This is the scenario that undermined the wetland project at Lake McCarrons, discussed in section 1 [*Oberts*, 1998; *Metropolitan Council*, 1997].

4.2.2. Nonstorm scenario 2. Next consider a system where the river has a sufficiently long residence time to reach its asymptotic state, that is, $r_R \approx 2WK\sqrt{A_W}/Q_r \geq 3$ (see Figure 7) and sun shading and wind sheltering are less prominent. These conditions are satisfied in large watersheds (large A_W) with a low annual discharge (small Q_r) and a wide river unobstructed by emergent vegetation, borderline trees, or hills. Unlike the previous scenario, a littoral wetland in such systems can produce little or no additional thermal mediation. Figure 10 illustrates the thermal cycles in one such system with $r_R = 3$. As shown on Figure 10a, the seasonal thermal cycles in the river, wetland, and lake are all at equilibrium with the atmosphere ($|\Delta T_i| \approx |\Delta T_E| = 15°C$ and $i = R, W, L$). However, since $\theta \rightarrow t_{\text{heat,ch}}$ in the limit $r \gg 1$ and $t_{\text{heat,ch}}/P \ll 1$ (see (19)), the lake ($t_{\text{heat,ch}} = 20$ days) lags the shallower river and wetland ($t_{\text{heat,ch}} = 1$–2 days) by 16–18 days. This produces a seasonal variation in intrusion depth, with the river and wetland inflow predominantly entering at the surface during J.D. = 20–200 when T_R and $T_W > T_L$ but are otherwise plunging. On diurnal and synoptic timescales (Figure 10b) the river and wetland heat and cool more rapidly than the lake, that is, $|\Delta T_W|$ and $|\Delta T_R| \gg |\Delta T_L|$. For the river with $t_{\text{heat,ch}} = 2$ days, the combined diurnal and synoptic temperature fluctuations are not large enough to produce variability in intrusion depth during a large fraction of the year, for example, $T_R < T_L$ throughout the time period on Figure 10b. For the wetland with $t_{\text{heat,ch}} = 1$ day, the larger-amplitude response (i.e., $|\Delta T_W| > |\Delta T_R|$) produces some variability in intrusion depth, for example, on J.D. = 254–257 and 264–267, during the 20 day period illustrated in Figure 10b. Despite this difference the intrusion depth dynamics of the river and the wetland are predominantly characterized by the seasonal variability, which is the same for both systems.

To summarize, a littoral wetland is less likely to alter the lake inflow dynamics in a watershed where the thermal capacity of the river system alone is sufficient to bring the water to its asymptotic state and where sun shading and wind sheltering are less prominent. The lake intrusion depth in such systems can vary on seasonal, synoptic, and/or diurnal timescales depending upon the specific system configurations.

4.2.3. Episodic events: Storms. Lake intrusion dynamics are of particular interest during storms, when nutrient and contaminant loads are peaking. Under these conditions the thermal evolution of surface water through the watershed differs significantly from the low-flow conditions described in sections 4.2.1 and 4.2.2. First, the source of river water switches from groundwater to surface runoff, which more closely reflects the current synoptic and seasonal atmospheric conditions. Second, the residence time in the river and the wetland drops significantly with the increased flow rates. This decreases their thermal capacity such that r_R and $r_W < 1$. Third, the wetland circulation becomes jet-dominated, and the associated short-circuiting further reduces its effective thermal capacity (see section 3.1). As a result, little thermal mediation occurs in the river or the wetland, and the temperature of the water reaching the lake reflects the prevailing synoptic meteorological conditions. In contrast, the lake does not respond to these short-term meteorological fluctuations because of its larger thermal inertia (recall from Figure 7, $|\Gamma|_{x=L} < 0.2$ for $t_{\text{heat,ch}}/P > 1$) but retains its balance with the seasonal conditions. Therefore, during storms the intrusion depth is governed by the prevailing meteorological conditions, which dictate the temperature of the lake inflow, and whether the prevailing conditions are warmer or colder than the seasonal conditions, which dictate the lake temperature. This result is useful in predicting the impact of storm contaminant fluxes on lake water quality, since it provides a simple tool for assessing

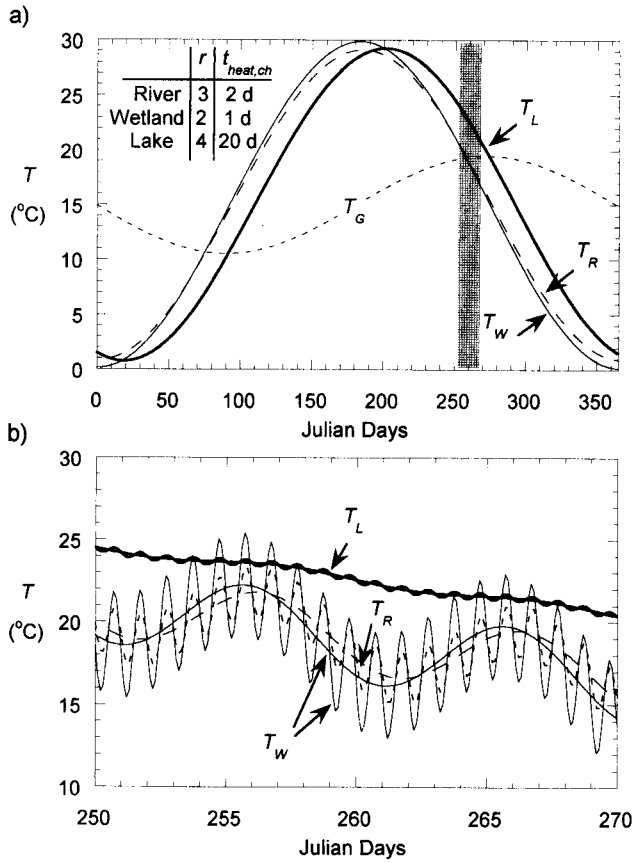

Figure 10. Nonstorm wetland impact scenario 2: $r_R = 3$. Dead-zone model solutions for a river, T_R, wetland, T_W, and lake epilimnion, T_L, originating from groundwater with the seasonal cycle $\bar{T}_G = 15°C$, $|T_G| = 5°C$, and $\theta_G = 3$ months [*Gu et al.*, 1996]. (a) Seasonal ($P = 365$ days) and (b) synoptic ($P = 10$ days) and diurnal ($P = 1$ day) responses. The addition of a littoral wetland does little to change the lake intrusion dynamics.

whether the inflow plunges (conditions are colder than seasonal average) or enters directly into the surface water (warmer than seasonal average).

5. Conclusions

Thermal mediation is a process through which shallow littoral regions, such as wetlands, forebays, or side arms, can control the initial fate of river-borne nutrient and contaminant fluxes within a lake or reservoir. As a river traverses these systems, the water temperature is modified through atmospheric heat exchange. The change in temperature can affect the intrusion depth and thus impact the lake water quality.

This paper provides a simple framework for evaluating the impact of these shallow littoral regions on the thermal characteristics of lake inflow. The dead-zone model, previously used for river routing and dispersion problems, is adapted to wetlands to predict thermal mediation under different meteorological conditions. The impact of the wetlands on lake inflow dynamics is then evaluated by integrating the wetland model into a watershed-scale analysis of surface water temperature, tracing the thermal evolution of the water from its source (runoff and/or groundwater), along the river reach, through the wetland, and finally within the lake. This watershed-scale perspective is a new approach necessary to study the interaction between the river, wetland, and lake. In addition, this approach for the first time describes the link between thermal mediation in shallow flow through systems and the previously studied process of differential heating and cooling.

Our analysis suggests that littoral wetlands can provide significant thermal mediation in watersheds, where the river water has not had enough time to equilibrate with the atmosphere or sun shading produces a different equilibrium temperature for the river than the lake. In such a system a wetland prolongs the time for heating/cooling during nonstorm conditions, reducing the seasonal temperature differences between the wetland outflow and lake. This makes the intrusion depth more sensitive to diurnal and synoptic meteorological fluctuations. Specifically, in summer the wetland can sufficiently raise the temperature of the lake inflow to produce a surface intrusion during the day, causing more river-borne nutrients and contaminants to enter directly into the epilimnion where they can potentially enhance eutrophication and human exposure to pathogens. This scenario was observed at Lake McCarrons, discussed in section 1 [*Oberts*, 1998; *Metropolitan Council*, 1997], and the Mystic Lake in Massachusetts (Andradóttir and Nepf, manuscript in preparation, 1999). A littoral wetland has less impact on lake intrusion dynamics in watersheds, where sun shading and wind sheltering are less prominent and the water has already reached thermal equilibrium with the atmosphere before reaching the wetland. Finally, nutrient and contaminant loads often peak during storms, making such events of particular interest to lake water quality. Our analysis suggests that during storms, wetland thermal mediation is less important and the intrusion depth is governed by the difference between current and seasonal meteorological conditions.

Appendix

The dead-zone model with $E^* = 0$ mimics a range of wetland circulation and thus does not limit the generality of the results presented in this paper. This can be seen by considering the product of the lateral exchange coefficient α^* and the jet areal ratio q:

$$\alpha^* q = \frac{\Delta Q}{(A_c + A_d)L}\frac{A_c L}{Q_r} = \frac{q\bar{t}}{(A_c + A_d)L/\Delta Q}$$

$$= \frac{\text{timescale of advection}}{\text{timescale of lateral exchange}}.$$

For $\alpha^* q \lesssim 1$, very little lateral exchange occurs in the timescale of advection, producing short-circuiting (Figure 2b). However if $\alpha^* q \gtrsim 1$, lateral exchange occurs at the same timescale as advection, and the balanced combination of differential advection (flow zone versus dead zone) and the lateral exchange creates longitudinal shear dispersion even if $E^* = 0$ [e.g., *Taylor*, 1954; *Chikwendu and Ojiakor*, 1985]. Finally, if $\alpha^* q \gg 1$, lateral exchange is much faster than advection, and the dead zone is no longer distinct from the flow zone, effectively producing plug flow through the entire area ($A_c + A_d$).

Acknowledgments. This work was funded by the National Institute of Environmental Health Sciences, Superfund Basic Research Program, grant P42-ES04675. The authors would like to thank Eric Adams for his valuable feedback throughout the development of this work and Chin Wu for his technical suggestions.

References

Adams, E. E., The transient response of cooling ponds, *Water Resour. Res.*, *18*(5), 1469–1478, 1982.

Andradóttir, H. Ó., Circulation and mixing in the upper forebay of the Mystic Lake system, Winchester, Massachusetts, Master's thesis, Mass. Inst. of Technol., Cambridge, 1997.

Babarutsi, S., J. Ganoulis, and V. H. Chu, Experimental investigation of shallow recirculating flows, *J. Hydraul. Eng.*, *115*(7), 906–924, 1989.

Bastian, R. K., and D. A. Hammer, The use of constructed wetlands for wastewater treatment and recycling, in *Constructed Wetlands for Water Quality Improvement*, edited by G. A. Moshiri, Lewis, Boca Raton, Fla., 1993.

Bencala, K. E., and R. A. Walters, Simulation of solute transport in a mountain pool-and-riffle stream: A transient storage model, *Water Resour. Res.*, *19*(3), 718–724, 1983.

Chikwendu, S. C., and G. U. Ojiakor, Slow-zone model for longitudinal dispersion in two-dimensional shear flows, *J. Fluid Mech.*, *152*, 15–38, 1985.

Day, T. J., Longitudinal dispersion in natural channels, *Water Resour. Res.*, *11*(6), 909–918, 1975.

DePaoli, L. L., Numerical modelling of wetland hydrodynamics, Master's thesis, Mass. Inst. of Technol., Cambridge, 1999.

Edinger, J. E., and J. C. Geyer, Heat exchange in the environment, *Publ. 65-902*, Edison Electr. Inst., New York, 1965.

Farrow, D. E., and J. C. Patterson, On the response of a reservoir sidearm to diurnal heating and cooling, *J. Fluid Mech.*, *246*, 143–161, 1993.

Fisher, H. B., E. J. List, R. C. Y. Koh, J. Imberger, and N. H. Brooks, *Mixing in Inland and Coastal Waters*, Academic, San Diego, Calif., 1979.

Gu, R., F. N. Luck, and H. G. Stefan, Water quality stratification in shallow wastewater stabilization ponds, *Water Resour. Bull.*, *32*(4), 831–844, 1996.

Harleman, D. R. F., Hydrothermal analysis of lakes and reservoirs, *J. Hydraul. Div. Am. Soc. Civ. Eng.*, *108*(HY3), 302–325, 1982.

Hutchinson, G. E., *A Treatise on Limnology*, John Wiley, New York, 1957.

Jirka, G. H., and M. Watanabe, Steady-state estimation of cooling pond performance, *J. Hydraul. Div. Am. Soc. Civ. Eng.*, *106*(HY6), 1116–1123, 1980.

Jirka, G. H., M. Watanabe, K. H. Octavio, C. F. Cerco, and D. R. F. Harleman, Mathematical predictive models for cooling ponds and lakes, Part A, Model development and design considerations, *Tech. Rep. 238*, Ralph M. Parsons Lab. for Water Resour. and Hydrodyn., Mass. Inst. of Technol., Cambridge, 1978.

Johnston, C. A., G. D. Bubenzer, G. B. Lee, F. W. Madison, and J. R. Mc Henry, Nutrient trapping by sediment deposition in a seasonally flooded lakeside wetland, *J. Environ. Qual.*, *13*(2), 283–290, 1984.

Kadlec, R. H., Detention and mixing in free water wetlands, *Ecol. Eng.*, *3*, 345–380, 1994.

Leopold, L. B., M. G. Wolman, and J. P. Miller, *Fluvial Processes in Geomorphology*, Dover, Mineola, N. Y., 1992.

Metropolitan Council, Lake McCarrons wetland treatment system–Phase III study report, *Publ. 32-97-026*, City of Roseville, Minn., 1997.

Mitsch, W. J., and J. G. Gosselink, *Wetlands*, Van Nostrand Reinhold, New York, 1993.

Monismith, S. G., J. Imberger, and M. L. Morison, Convective motions in the sidearm of a small reservoir, *Limnol. Oceanogr.*, *35*(8), 1676–1702, 1990.

Oberts, G. L., Long-term reductions in removal effectiveness: Lake McCarrons wetland treatment system, paper presented at ASCE Wetlands Engineering and River Restoration Conference, Am. Soc. of Civ. Eng., Denver, Colo., 1998.

Reed, S. C., and D. S. Brown, Constructed wetland design–The first generation, *Water Environ. Res.*, *64*(6), 776–781, 1992.

Ryan, P. J., D. R. F. Harleman, and K. D. Stolzenbach, Surface heat loss from cooling ponds, *Water Resour. Res.*, *10*(5), 930–938, 1974.

Sinokrot, B. A., and H. G. Stefan, Stream temperature dynamics: Measurements and modeling, *Water Resour. Res.*, *29*(7), 2299–2312, 1993.

Taylor, G. I., Dispersion of soluble matter in solvent flowing slowly through a tube, *Proc. R. Soc. London, Ser. A*, *223*, 446–468, 1954.

Tchobanoglous, G., Constructed wetlands and aquatic plant systems: Research, design, operational and monitoring issues, in *Constructed Wetlands for Water Quality Improvement*, edited by G. A. Moshiri, Lewis, Boca Raton, Fla., 1993.

Thackston, E. L., F. D. Shields Jr., and P. R. Schroeder, Residence time distributions of shallow basins, *J. Environ. Eng.*, *113*(6), 1319–1332, 1987.

Valentine, E. M., and I. R. Wood, Longitudinal dispersion with dead zones, *J. Hydraul. Div. Am. Soc. Civ. Eng.*, *103*(HY9), 975–990, 1977.

Wood, A., Constructed wetlands in water pollution control: Fundamentals to their understanding, *Water Sci. Technol.*, *32*(3), 21–29, 1995.

Wu, J., and I. K. Tsanis, Pollutant transport and residence time in a distorted scale model and numerical model, *J. Hydraul. Res.*, *32*(4), 583–598, 1994.

Yotsukura, N., A. P. Jackman, and C. R. Faust, Approximation of heat exchange at the air-water interface, *Water Resour. Res.*, *9*(1), 118–128, 1973.

Yu, Y. S., and L. Wenzhi, Longitudinal dispersion in rivers: A dead-zone model solution, *Water Resour. Bull.*, *25*(2), 319–325, 1989.

H. Ó. Andradóttir and H. M. Nepf, Ralph M. Parsons Laboratory, Department of Civil and Environmental Engineering, Massachusetts Institute of Technology, Room 48-114, Cambridge, MA 02139. (hoa@mit.edu; hmnepf@mit.edu)

(Received March 8, 1999; revised October 5, 1999; accepted October 13, 1999.)